EJECTED BOULDERS: IMPLICATIONS FOR SECONDARY CRATERS AND THE AGE DATING OF SURFACES.
Gwendolyn D. Bart, H. J. Melosh, *Univ. of Arizona, 1629 E. University Blvd., Tucson, AZ 85721, USA, (gwenbart@lpl.arizona.edu)*.

Introduction

The size-frequency distribution (SFD) of craters on the Moon, Mars, and Mercury turns up at very small crater diameters; for the Moon the upturn occurs near 3 km [1, 2]. Neukum, Ivanov, and Hartmann [2] propose that this upturn is a result of collisional process in the asteroid belt and represents the impacting population. On the other hand, Shoemaker [3] and others [1, 4, 5] propose that this upturn is a result of secondary cratering, wherein solid material ejected from an impact crater itself impacts the surface, forming a crater.

Secondary craters are formed from solid blocks (or groups of blocks) ejected from impact craters. Therefore, to better understand whether secondary craters cause this upturn in the SFD, we examined ejected boulders scattered around four small craters — three on the Moon and one on Mars. We compare the observed distribution of these boulders to the distribution of secondary craters around large primary craters. Lee et al. [6] also examined boulders ejected from craters and constructed size-frequency plots, though they do not specifically address the issue regarding secondaries and the SFD.

Cumulative Plots

We measured the size and location of more than 7,000 boulders apparently ejected from craters on the Moon and Mars using data from *Lunar Orbiter III* and *Mars Global Surveyor*. We plotted boulder diameters from one crater (observed in *Lunar Orbiter III* image 185 H 3 of 3) on a cumulative plot (Fig. 1, as described in [7]). At each diameter we plot the total number of boulders that size *and bigger*. The plot shows that the $10^{3.2} (\simeq 1550)$ boulders have diameters ranging from $10^0 (\simeq 1)$ m to $10^{1.15} (\simeq 14)$ m. Most of these boulders fall roughly along a line of slope -4. At the smallest boulder diameters the plot flattens out, which we attribute to resolution effects; small boulders are more difficult to identify and measure. The resolution of this image was 0.3 m/pixel.

Shoemaker [3] discusses in detail primary and secondary cratering on the lunar surface. His paper is based on the *Ranger VII* photographs that revealed for the first time features smaller than 300 m on the Moon. He discusses several cumulative plots of lunar craters on the Mare Cognitum. He showed that cumulative plots that include all craters (regardless of whether they are primary or secondary) lie along a line of slope a bit more shallow than -2. However, he finds that when cumulative plots are made which only include secondary craters, the data lie along a slope of about -4.

On a cumulative plot, our boulders also plot along a slope close to -4 (Fig. 1). This similarity is most likely not a coincidence; we propose that these boulders did not create secondaries simply because the primary impact had insufficient energy to eject these boulders at velocities high enough to form secondary craters.

Interestingly, we did identify eight secondary craters around one 500 m diameter crater on the Moon. They lie about 2.5 crater radii from the rim. These few secondary craters lie amid the several thousand boulders surrounding the crater. The blocks which formed them may have been ejected from the crater early in the crater formation process at high speeds and steep angles, providing them with enough energy to form secondary craters among other blocks that just came to rest on the surface.

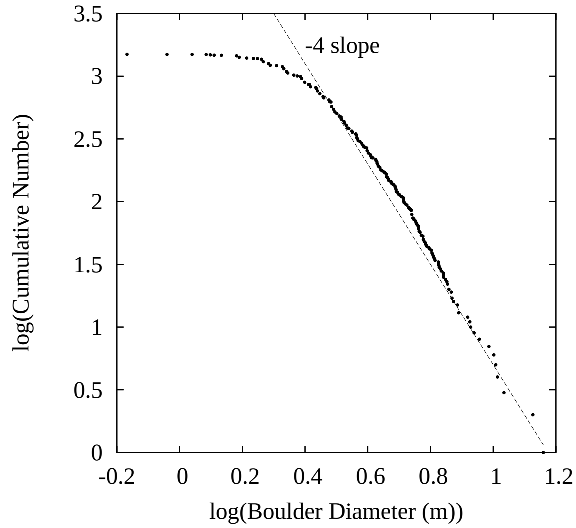

Figure 1: A log-log cumulative plot of boulders from a lunar crater observed in *Lunar Orbiter III* image 185H 3 of 3. A line of slope -4 is also plotted for comparison.

Size-Ejection Velocity Relation

Other studies [8, 9] have performed size-ejection velocity studies of secondary craters; we performed a similar analysis for boulders. First we measured the distance from the center of the crater to each boulder. Then we used that distance to calculate the ejection velocity.

To present our data (Fig. 2) we indicate via grayscale a value which reflects the concentration of boulders in that region of the plot; darker indicates more boulders. The values are a sum of the "distances" on the plot from a particular location on the graph to each boulder, weighted by a Gaussian: $\sum_{i=1}^{n} \exp\left(-\frac{1}{2}\left(\frac{r_i}{\sigma}\right)^2\right)$, where n is the number of boulders, r_i is the distance to the ith boulder, and σ is 0.10.

All four craters showed similar patterns; Fig. 2 is an example of boulders around a 300 m diameter lunar crater observed in *Lunar Orbiter III* image 185 H 3 of 3. Larger boulders (1.8 to 3.0 m radius) are found closer to the crater center, within $\sim$500 m. In the plot, boulders are concentrated around the region of 1.2 m radius and 350 m from the crater center (205 m

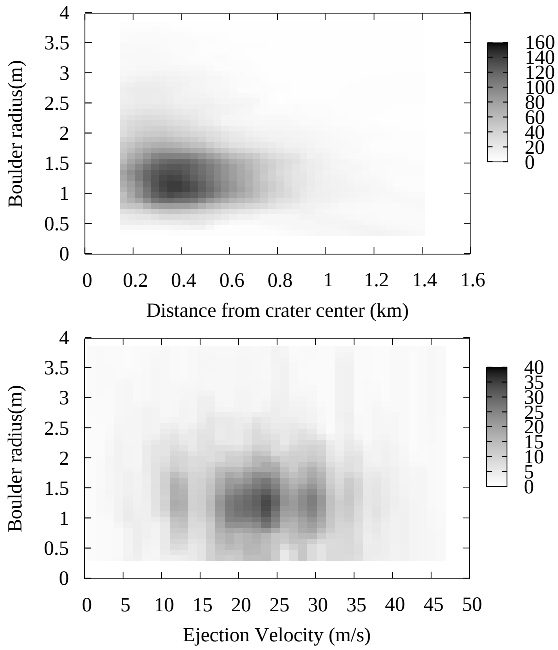

Figure 2: (upper) A plot of distance (from the crater center to the boulder) versus radius of the boulder. (lower) A plot of boulder ejection velocity versus radius of the boulder. In both cases the darker regions indicate more data points in that area of the graph; see text for precise explanation.

from the crater rim.) Also, boulders with a radius smaller than ~ 0.50 m are near the limit of resolution and so fewer boulders were identified in that region.

The boulder's probable ejection velocity was then calculated; Fig. 3 illustrates the various parameters involved in this calculation. The total distance, D, from the crater center to the boulder must equal the distance from the crater center to where the boulder was ejected from, r, plus the distance that the boulder flew, f. We assume the boulder followed a ballistic path, with the distance it flew being determined by its velocity (v), the gravity (g), and the ejection angle (ϕ): $f = \frac{v^2}{g} \sin 2\phi$, where ϕ was assumed to be $\sim 45^\circ$. The ejection velocity can also be calculated from scaling laws [10, 11], where it depends on the transient radius of the crater, R, the gravity of the body, g, and the strength of the target material, ϵ. From these parameters we determine numerically the ejection velocity of each boulder and where each boulder was ejected from within the crater. We present the ejection velocity data in Fig. 2.

Although the boulder radius does seem to depend on distance from the crater, the ejection velocity does not. This is different than what Vickery [8] found, where fragment size depended strongly on ejection velocity. In that case though, the ejection velocities and fragment sizes being dealt with were three orders of magnitude greater than the values from these small craters. It is possible that the significantly smaller craters examined in this study exhumed blocks that were formed along preexisting fractures, generating a fairly flat ejection velocity plot. Large craters such as those examined by Vickery [8] had

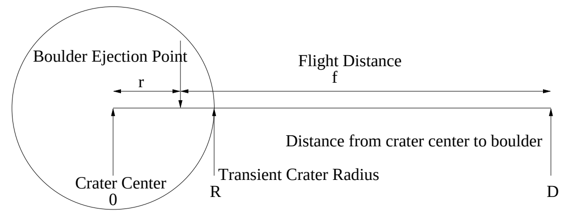

Figure 3: Diagram explaining variables in the ejection velocity equations.

sufficient energy to fracture the target and throw out boulders whose size was correlated to the velocity at which they were ejected.

Conclusion

We characterized boulders around four craters on the Moon and Mars and compared the results with other studies of secondary craters. Our cumulative SFD plot for boulders has a slope of -4, similar to that which Shoemaker [3] found for secondary craters. Because of the genetic relationship between boulders and secondary craters, this result supports the hypothesis of Shoemaker and others that the upturn of the SFD at small crater sizes is a result of secondary impacts. The size-ejection velocity relation of our boulders shows that larger boulders are preferentially found closer to the crater, but that ejection velocity does not appear to be strongly dependent on boulder size. Our result differs from that obtained by Vickery [8] for secondary craters, although we are looking at features several orders of magnitude smaller. Understanding the distributions of boulders around small craters is an important step in understanding the nature of small scale cratering on planetary bodies, and will affect the way that surface cratering ages are determined.

References

[1] Soderblom, L. A., Condit, C. D., West, R. A., Herman, B. M., and Kreidler, T. J. *Icarus* **22**, 239–263 July (1974). [2] Neukum, G., Ivanov, B. A., and Hartmann, W. K. *Space Science Reviews* **96**, 55–86 April (2001). [3] Shoemaker, E. M. In *The Nature of the Lunar Surface*, (1965). [4] Brinkmann, R. T. *J. Geophys. Res.* **71**(1), 340–342 January (1966). [5] Bierhaus, E. B., Chapman, C. R., Merline, W. J., Brooks, S. M., and Asphaug, E. *Icarus* **153**, 264–276 October (2001). [6] Lee, S. W., Thomas, P., and Ververka, J. *Icarus* **68**, 77–86 October (1986). [7] Arvidson, R. E., Boyce, J., Chapman, C., Cintala, M., Fulchignoni, M., Moore, H., Neukum, G., Schultz, P., Soderblom, L., Strom, R., Woronow, A., and Young, R. *Icarus* **37**, 467–474 February (1979). [8] Vickery, A. M. *Icarus* **67**, 224–236 August (1986). [9] Hirase, Y., Nakamura, A. M., and Michikami, T. *Planet. Space Sci.* **52**, 1103–1108 October (2004). [10] Schmidt, R. M. and Holsapple, K. A. *Geol. Soc. Amer. Spec. Pap.* **190**, 93–102 (1982). [11] Holsapple, K. A. and Schmidt, R. M. *J. Geophys. Res.* **72**, 1849–1870 (1982).